Time-resolved nanoseconds dynamics of ultrasound contrast agent microbubbles manipulated and controlled by optical tweezers

Valeria Garbin*[a,b], Dan Cojoc[a], Enrico Ferrari[a,b], and Enzo Di Fabrizio[c,a]
[a]CNR-INFM, Laboratorio Nazionale TASC, S.S. 14 km 163.5, 34012 Trieste, Italy
[b]Department of Physics, University of Trieste, via Valerio 2, 34027 Trieste, Italy
[c]"Magna Græcia" University of Catanzaro, v.le Europa, 88100 Germaneto (CZ), Italy

Marlies Overvelde[d], Michel Versluis[d], Sander van der Meer[d], Nico de Jong[d,e], and Detlef Lohse[d]
[d]Physics of Fluids,University of Twente, P.O. Box 217, 7500 AE Enschede, The Netherlands
[e]Exp. Echocardiography, Thoraxcentre, Erasmus MC, Rotterdam, The Netherlands

ABSTRACT

Optical tweezers enable non-destructive, contact-free manipulation of ultrasound contrast agent (UCA) microbubbles, which are used in medical imaging for enhancing the echogenicity of the blood pool and to quantify organ perfusion. The understanding of the fundamental dynamics of ultrasound-driven contrast agent microbubbles is a first step for exploiting their acoustical properties and to develop new diagnostic and therapeutic applications. In this respect, optical tweezers can be used to study UCA microbubbles under controlled and repeatable conditions, by positioning them away from interfaces and from neighboring bubbles. In addition, a high-speed imaging system is required to record the dynamics of UCA microbubbles in ultrasound, as their oscillations occur on the nanoseconds timescale.
In this work, we demonstrate the use of an optical tweezers system combined with a high-speed camera capable of 128-frame recordings at up to 25 million frames per second (Mfps), for the study of individual UCA microbubble dynamics as a function of the distance from solid interfaces.

Keywords: diffractive optical elements, optical tweezers, Laguerre-Gaussian beam, optical vortex, low-index particle, ultrasound contras agent, microbubble, high speed imaging

1. INTRODUCTION

Optical vortices have proven to be a powerful tool for 3D trapping and non-contact manipulation of low-refractive index microscopic particles [1], which cannot be trapped by conventional optical tweezers based on a focused Gaussian beam [2]. This observation has recently found important applications for the study of ultrasound contrast agent (UCA) microbubbles [3], which are used in ultrasound medical imaging for enhancing the visibility of blood vessels and organ perfusion. The ability to control the position of bubbles relative to rigid interfaces, and relative to neighboring bubbles, is crucial for overcoming the most common problem when studying UCA microbubbles: due to buoyancy, they rise up to the walls of chamber or capillaries where they are injected, and they stick together forming bubble clusters. The acoustic behavior of bubbles with such non-controlled and non-repeatable boundary conditions is expected to be different than the behavior of a totally free bubble, oscillating away from interfaces and other bubbles. Here we demonstrate the applicability of optical trapping for studying UCA microbubbles with controlled boundaries, by positioning them at prescribed distance from the chamber wall prior to insonation with ultrasound. The optical tweezers setup is combined with the high speed camera Brandaris 128 [4] for recording the UCA microbubble dynamics with sub-μs temporal resolution.

1.1. Manipulation of single and multiple UCA microbubbles

Different methods can be implemented for generating traps for low-index particles: two-dimensional trapping can be performed by using an interferometric pattern of bright and dark fringes [5], by generating donut-shaped intensity

Optical Trapping and Optical Micromanipulation III, edited by Kishan Dholakia, Gabriel C. Spalding,
Proc. of SPIE Vol. 6326, 63261V, (2006) · 0277-786X/06/$15 · doi: 10.1117/12.680576

distributions using the generalized phase-contrast method [6], or by using a Bessel beam [7]. Three-dimensional trapping can be obtained by rapidly scanning the beam in a circular trajectory [8] or by focusing an optical vortex beam, e.g. a Laguerre-Gaussian beam. Beams containing an optical vortex can be generated by converting a Gaussian beam through either amplitude or phase-only [9] diffractive optical elements (DOEs). Arrays of traps for confining multiple microbubbles can also be generated using diffractive optical elements, following two approaches: the two phase masks which generate the optical vortex and split the beam into several beams, respectively, can be superimposed [10]; alternatively, the DOE can be divided into several sections, each one containing a single-vortex phase mask [11]. Either way, by implementing the DOEs on a spatial light modulator (SLM) the configuration of traps can be modified in real-time enabling full control on the number of trapped bubbles and on the bubble-to-bubble distance. In this work we generate two-vortex phase masks by using the second approach [11], which will be applied to the study of the bubble-to-bubble interaction.

1.2. High speed imaging

Optical recordings of UCA microbubbles dynamics upon insonification require a sampling rate in the million frames per second (Mfps) range, to allow accurate representation of the oscillation period and amplitude. In addition, more than 100 frames are desirable as the ultrasound typically lasts for 10 cycles during which the response of the microbubbles can be highly non-linear, and the number of frames should be sufficient to record the whole process. In this work, high speed imaging is performed using a digital rotating mirror camera, specifically developed to investigate microbubble dynamics, capable of 128-frame recordings at 25 Mfps [4]. Previous studies performed with this instrument were carried out by confining the microbubbles in space either by injection in a soft, acoustically transparent capillary [12] or by producing bubbles in a rising train [13]. Even though soft capillaries do not scatter ultrasound, their walls do affect bubble dynamics; in addition, the effect of neighboring bubbles may not be negligible. The use of optical tweezers for controlling the position of UCA microbubbles overcomes these limitations.

2. EXPERIMENTAL SETUP AND METHODS

Our setup combines an optical tweezers system based on an upright microscope and a spatial light modulator, with the high speed camera Brandaris 128. The camera is connected to the output port of the microscope.

The setup for optical trapping (Fig. 1) is based on a upright microscope (BXFM, Olympus). The Gaussian beam coming from a 1064 nm CW Yb fiber laser (YLM, IPG Photonics) is converted into a Laguerre-Gaussian mode upon reflection on the phase diffractive optical element implemented on a spatial light modulator (X8267-11, Hamamatsu). The beam is then resized by a telescope (lenses L_1, L_2) to fit the objective entrance pupil. A dichroic mirror (CVI Laser) reflects the beam into the 100× microscope objective (LUMPLFL, Olympus; NA = 1.00, water immersion). The Laguerre-Gaussian beam is then focused into a sample cell. Transmission imaging is performed either in real time on a CCD camera (LCL-902HS, Watec), or at high speed using the Brandaris 128 camera. A beam splitter (BS) transmits 20% of the incident light to the CCD, and reflects the remaining 80% into the high speed camera. Beam shape and position can be monitored on the CCD, while an IR filter (CVI Laser) is inserted in the path of the high-speed camera to block any residual laser light coming through the dichroic mirror.

A small water container with an unfocused 2.25 MHz transducer (V306, Panametrics Inc.) is mounted on a (*x, y, z*) micropositioning stage located below the objective. The transducer is mounted at 45° incidence angle with the optical axis, so that the acoustical field overlaps the optical focal volume. The sample cell is an OptiCell cell culture chamber (BioCrystal, Inc.), which is formed by two polystyrene-matrix material membranes of 75 µm thickness positioned at 2 mm spacing, and it is placed perpendicular to the optical axis into the overlap region. In previous experiments [14], the membranes were observed to exhibit optimum optical and acoustical transmission. The chamber volume (10 ml) is filled with a degassed 0.9% NaCl aqueous solution prior to UCA microbubble injection. All studies are performed with the experimental contrast agent BR-14 (Bracco Research S.A.), which is a phospholipid-stabilized agent comprising of perfluorobutane-filled microbubbles; 99% of the bubbles have diameters less than 10 µm according to the manufacturer's specifications. The bubble density is optimized to have up to 5-10 bubbles in the field of view of the camera.

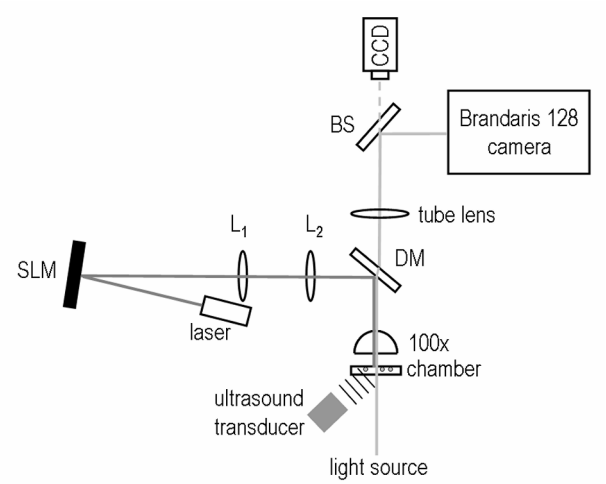

Fig. 1: Optical setup for combined UCA microbubble trapping and high speed imaging. The laser beam is reflected by the spatial light modulator (SLM) and resized by a telescope (lenses L_1 and L_2); it enters the objective (100x) upon reflection on a dichroic mirror (DM) and is focused into the sample volume. Imaging is achieved by illuminating the sample in transmission. The image is formed by the microscope tube lens at the primary image plane of the high-speed camera, and a beam splitter (BS) enables simultaneous monitoring on a CCD camera.

DOEs are calculated which generate a Laguerre-Gaussian beam with an appropriate size in the objective's focal plane for trapping bubbles with resting radius R_0 between 1 and 3 μm. This range for the bubble size is determined by the ultrasound frequency available from the transducer (2.25 MHz), as they have resonance frequency close to this value. In our setup Laguerre-Gaussian beams with topological charge between 6 and 8 are found to have the appropriate size for this range of bubble radii. Bubbles are stably trapped in 3D in a position 20-30 μm below the objective's focal plane. In order to compensate for this mismatch (so as to have the trapped bubble in focus), the trap position is moved by changing the distance between lenses L_1, L_2. The beam then enters the objective with a slight convergence, thereby effectively lifting the trapping plane to coincide with the objective's focal plane.

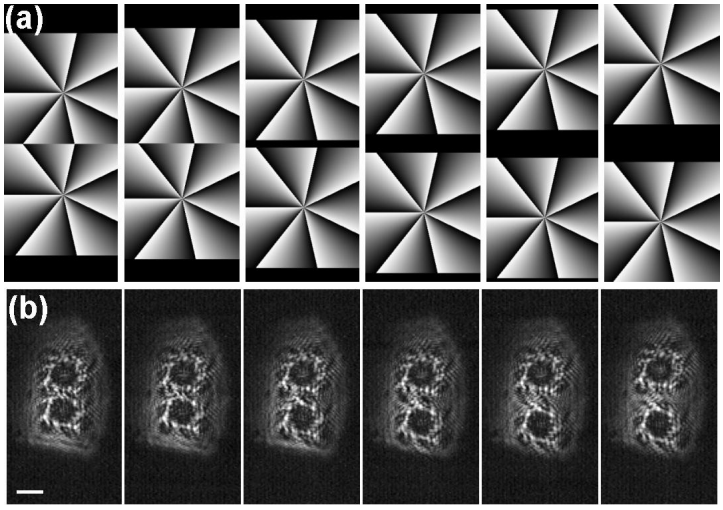

Fig. 2: two Laguerre-Gaussian beams (b) are produced using tiled DOEs (a). The distance between the two traps can be controlled by changing the distance between the singularities in the DOE plane. White scalebar left bottom in (b): 5 μm.

DOEs for two Laguerre-Gaussian traps are also generated by juxtaposing two single-trap DOEs [11]. The 768×768 pixels DOEs which generate a single trap are resized so that two of them fit in the SLM's active area (768×768 pixels). The distance between the two juxtaposed DOEs can be adjusted to change the distance between the two traps, as shown in Fig. 2. This will enable a detailed study on the bubble-to-bubble interactions as a function of their distance. Trapping of two UCA microbubbles using such a configuration of traps is demonstrated in Fig. 3. Each one of the two bubbles can be individually sorted, by switching on one trap at a time.

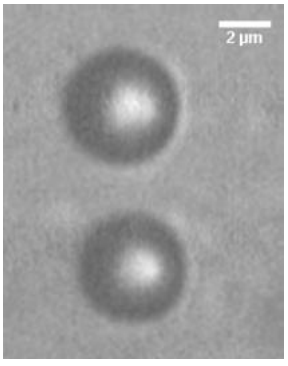

Fig. 3: two bubbles are trapped using the two-trap DOE. The distance between the bubbles can be controlled dynamically by changing the distance between the traps, as it is shown in Fig. 2. Scalebar 2 µm.

Triggering of the experiment is crucial to obtain movies of oscillating bubbles in focus. Before each recording the laser is blocked to prevent optical radiation forces from affecting the bubble dynamics. A photodiode is used to detect the laser blockage and triggers the ultrasound pulses and the recordings. The released bubble starts floating upwards, to the chamber wall, due to buoyancy. The terminal rise velocity of a buoyant bubble in water can be evaluated, assuming no slip, from [15]:

$$v_{Stokes} = \frac{4R^2(\rho_{water} - \rho_{air})}{18\eta_{water}} \quad (1)$$

where ρ_{water} = 1.01 10^{-3} N s m^{-2} is the viscosity of water at 20°C, ρ_{water} = 1000 kg m^{-3} the density of water and ρ_{air} = 1 kg m^{-3} the density of air. For a 3 µm radius bubble the terminal velocity is then about 20 µm s^{-1}. As the maximum time between the triggering and the recording is of the order of 50 ms, the biggest bubbles rise up by no more than 1 µm. This distance is smaller than the objective's depth of focus (2 µm), so that the bubble is still in focus during the recording. Furthermore, as the laser is blocked only for a few tens of milliseconds during the time of the recoding, the bubble is still in the trap after the experiment. In this way, multiple experiments can be performed on the same bubble and its behavior under different experimental conditions can be studied.

3. RESULTS

The setup presented in § 2 allows the selection of an individual bubble and trap it with 3D control over its position from the top wall of the sample chamber. After trapping, the vertical position of the bubble is finely adjusted by tuning the laser power, to ensure that the bubble is in the microscope objective's focal plane. The bubble is then positioned at a prescribed distance from the wall by lifting the chamber using the micropositioning stage, see Fig. 4. The typical insonation protocol is a 8-cycles ultrasound burst at 2.25 MHz, with an applied pressure of 150 to 200 kPa.

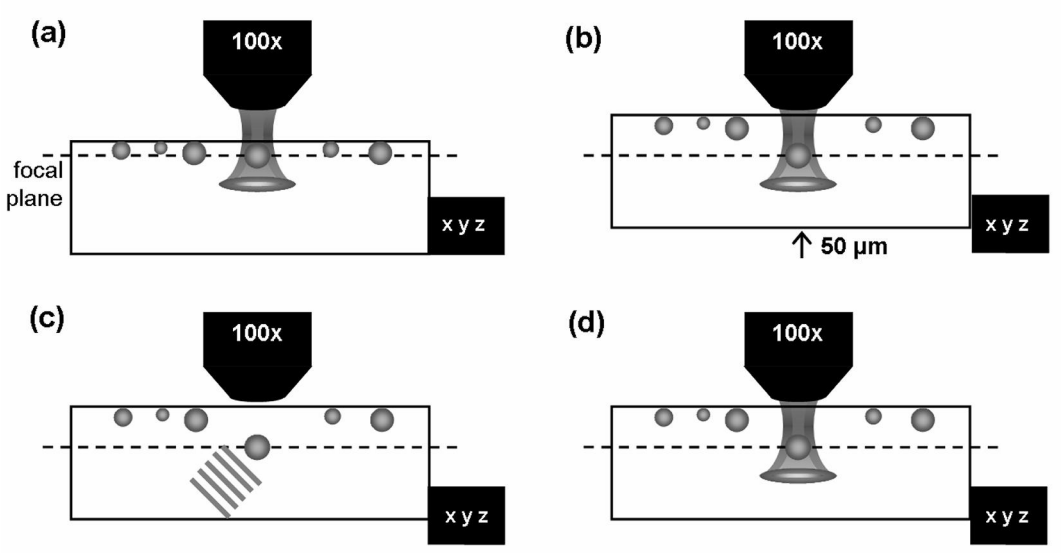

Fig. 4: Schematic of an experiment. (a) The bubble to be studied is selected and trapped. (b) The camber is lifted with a micropositioning stage, so that the distance from the wall can be precisely controlled. The position of the microbubble relative to the microscope objective's focal plane is adjusted, if necessary, by tuning the laser power. (c) The laser is blocked during insonation with ultrasound and recording of the bubble response. (d) The laser is unblocked after the recording, so that the bubble is still in the trap and more experiments can be repeated on the same bubble.

We positioned individual microbubbles 50 µm away from the wall and recoded their dynamics upon insonation with ultrasound at 15 Mfps, see Fig. 5. Repeated measurements could be performed on the same bubble, as it was always found back in the trap after the laser was unblocked. This system is thus a reliable one for performing experiments and comparing the behavior of a microbubble under different conditions. Operating at 15 Mfps the temporal resolution of the high speed camera was 65 ns (Fig. 5).

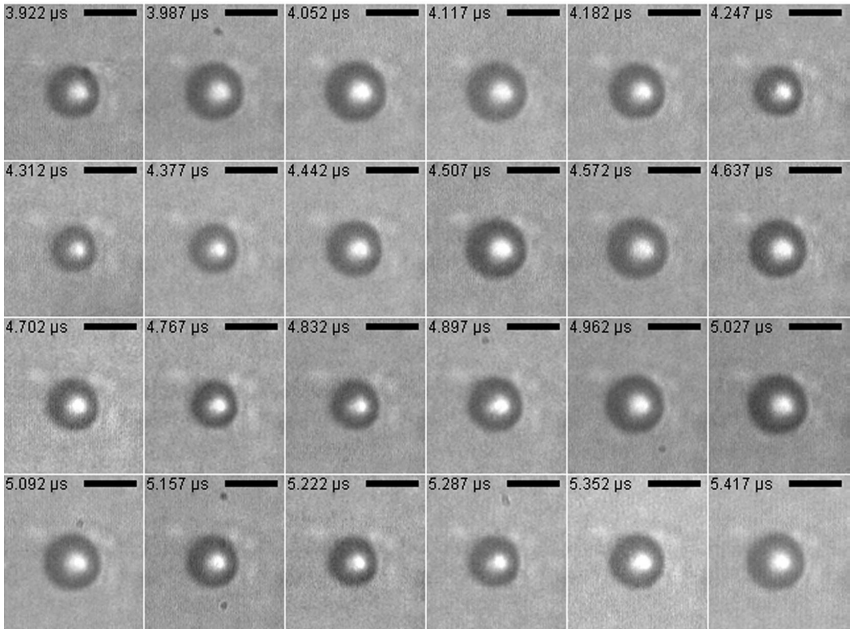

Fig. 5: UCA microbubble positioned 50 µm away from the sample chamber wall, freely oscillating at 2.25 MHz, recorded at 15.43 Mfps. In figure, 24 of the 128 frames are shown. The interframe time is 65 ns. Scalebar 5 µm.

Movies of 128 frames each are recorded and processed with a tracking algorithm to extract the radial excursion as a function of time. The resulting radius-time curves are compared with theoretical models and numerical simulations of the bubble dynamics [16-18]. A radius-time curve obtained for a 2.25 µm bubble is shown in Fig. 6.

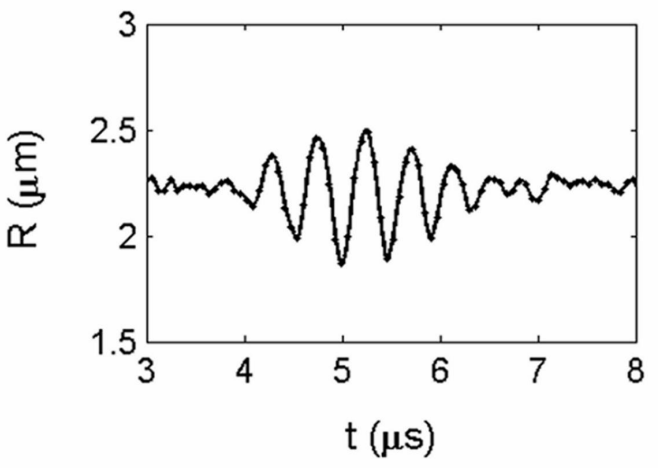

Fig. 6: Bubble radius oscillations upon insonification (ultrasound burst of 8 cycles at a frequency of 2.25 MHz). The radius-time curve is obtained by tracking the bubble in the 128 frames of a movie (92 of the 128 data points are shown here).

4. CONCLUSIONS

A setup was described that allows time-resolved optical monitoring of ultrasound contrast agent microbubble dynamics under ultrasound insonation, with controlled boundary conditions. A digital rotating mirror high-speed camera resolves in a sub-μs timescale the bubble oscillation dynamics. Coupling of this instrument to an optical tweezers setup allows the manipulation of microbubbles, such that controlled boundary conditions for the oscillating bubbles can be achieved. Recordings of individual, freely oscillating microbubbles were presented, obtained at a 15 Mfps frame rate.

Studying the dynamics of free oscillations is the first step in understanding bubble behavior; in the future the combined setup will be exploited to optically investigate bubble dynamics as a function of distance from interfaces. A study of the acoustical behavior as a function of bubble distance from interfaces may provide new diagnostic opportunities, if confirmed that free flowing bubbles can be acoustically discriminated from those which have bound to target cells, such as functionalized microbubbles designed for target-specific imaging and therapeutic applications.

In addition, dynamic implementation of diffractive optical elements on a programmable spatial light modulator will enable further studies on bubble-to-bubble interactions. Multiple bubbles can not only be trapped and manipulated by multiple Laguerre-Gaussian beams, but their spatial configuration can also be changed in real time by displaying a sequence of DOEs.

ACKNOWLEDGEMENTS

We acknowledge Bracco Research S.A. (Geneva) for supplying the contrast agent (BR-14). In particular, we would like to thank Marcel Arditi and Peter Frinking of Bracco Research S.A. for initiating this work and for their helpful comments, and Marco Mattiuzzi of Bracco Imaging (Milan). Bracco Imaging is acknowledged for supporting V.G. with a PhD grant. We are grateful to Miltcho Danailov of Elettra (Trieste) for helpful advices and to Federico Salvador and Stefano Bigaran of TASC (Trieste) for technical support. We thank Annemieke van Wamel and Marcia Emmer of Erasmus MC Rotterdam and Jos de Jong of University of Twente for support and assistance. We highly appreciate the skillful technical assistance of Frits Mastik, Jan Honkoop, Leo Bekkering, Cees Pakvis and Wim van Alphen of Erasmus MC Rotterdam and Gert-Wim Bruggert, Martin Bos and Bas Benschop of the University of Twente.

REFERENCES

1. K.T. Gahagan and G.A. Swartzlander, “Optical vortex trapping of particles”, *Opt. Lett.* 21, 827-829 (1996); K.T. Gahagan and G.A. Swartzlander, “Trapping of low-index microparticles in an optical vortex”, *J. Opt. Soc. Am. B* 15, 524-534 (1998)
2. A. Ashkin, “Forces of a single-beam gradient trap on a dielectric sphere in the ray optics regime”, *Biophys. J.* 61, 569-582 (1992)
3. P. Prentice, A. Cuschieri, K. Dholakia, M. Prausnitz, P. Campbell, “Membrane disruption by optically controlled microbubble cavitation”, *Nat. Phys.* 1, 107-110 (2005)
4. C.T. Chin, C. Lancée, J. Borsboom, F. Mastik, M.E. Frijlink and N. de Jong, M. Versluis and D. Lohse, “Brandaris 128: A digital 25 million frames per second camera with 128 highly sensitive frames”, *Rev. Sci. Instr.* 74, 1-9 (2003)
5. M.P. McDonald, L. Paterson, W. Sibbet, K. Dholakia, “Trapping and manipulation of low-index particles in a 2-dimensional interferometric optical trap”, *Opt. Lett.* 26, 863-865 (2001)
6. V.R. Daria, P.J. Rodrigo, J. Glückstad, “Real-time interactive optical micromanipulation of a mixture of high- and low-index particles ”, *Opt. Express* 12, 1417-1425 (2004)
7. V. Garcés-Chávez, D. McGloin, H. Melville, W. Sibbett, and K. Dholakia, “Simultaneous micromanipulation in multiple planes using a self-reconstructing light beam”, *Nature* 419, 145-147 (2002)
8. K. Sasaki, M. Koshioka, H. Mishawa, N. Kitamura, and H. Masuhara, “Optical trapping of a metal particle and a water droplet by a scanning laser beam”, *Appl. Phys. Lett.* 60, 807-809 (1992)
9. H. He, N. R. Heckenberg and H. Rubinsztein-Dunlop, “Optical particle trapping with higher-order doughnut beams produced using high efficiency computer generated holograms”, J. Mod. Opt. 42, 217-223 (1995)

10. J.E. Curtis, B.A. Koss, D.G. Grier, “Dynamic holographic optical tweezers”, *Opt. Commun.* 207, 169-175 (2002)
11. N. Chattrapiban, E.A. Rogers, I.V. Arakelian, R. Roy, W.T. Hill, “Laser beams with embedded vortices: tools for atom optics”, *J. Opt. Soc. Am. B* 23, 94-103 (2006)
12. A. Bouakaz, M. Versluis, N. De Jong, “High-speed optical observations of contrast agent destruction”, *Ultrasound in Med. & Biol.* 3, 391-399 (2005)
13. P. Palanchon, P. Tortoli, A. Bouakaz, M. Versluis and N. De Jong, “Optical observations of acoustical radiation force effects on individual air bubbles”, *IEEE Trans. Ultrasound Ferroel. Freq. Control* 52, 104-110 (2005)
14. A. van Wamel, A. Bouakaz, M. Versluis, N. de Jong, “Micromanipulation of endothelial cells: Ultrasound-microbubble-cell interaction”, Ultrasound in Med. and Biol. 30, 1255-1258 (2004)
15. S.H. Lamb, Hydrodynamics, 6th ed. (New York: Dover, 1993)
16. M. S. Plesset, A. Prosperetti, “Bubble Dynamics and Cavitation”, *Annu. Rev. Fluid. Mech.* **9**, 145-185 (1977).
17. C. E. Brennen, Cavitation and Bubble Dynamics (Oxford University Press: Oxford, 1995).
18. M. Brenner, S. Hilgenfeldt, D. Lohse, "Single bubble sonoluminescence", *Rev. of Mod. Phys.* **74**, 2, 425-484 (2002).